

# Durability design of composite pultruded profiles

## Design para a durabilidade de perfis compósitos pultrudidos

P. Brandão<sup>1</sup> | A. Pais<sup>1</sup> | M. Figueiredo<sup>1</sup> | R. Guedes<sup>1</sup> | A. T. Marques<sup>1</sup>

<sup>1</sup>Faculdade de Engenharia da Universidade do Porto, Rua Dr. Roberto Frias, s/n 4200-465 Porto, Portugal

### abstract

This work studies the durability of composite pultruded profiles, aiming for an approach of a designer to increase the in-service lifetime of a pultruded glass fiber reinforced polymer (pGFRP) profiles. Experimental three-point bending tests were done to obtain the properties of the material. Then, short-term creep tests at high loading levels measured the time to failure of the profile. The creep compliance of the profile was well captured by linear Findley's model. Finally, the influence of water absorption was assessed using short-term creep tests.

**Keywords:** Pultrusion, Composite profiles, Creep, Durability

### resumo

Neste trabalho estudou-se a durabilidade de perfis compósitos pultrudidos com o objetivo de aumentar o tempo de vida útil de perfis de polímero reforçado com fibra de vidro obtidos por pultrusão. As propriedades do material foram medidas através de ensaios experimentais de flexão em três pontos. Em seguida, foram realizados ensaios de fluência de curta duração com cargas elevadas para determinar os tempos até à rotura. A flexibilidade de fluência do perfil foi representada por um modelo de Findley. Finalmente, avaliou-se a influência da absorção de água através de ensaios de fluência de curta duração.

**Palavras-chave:** Pultrusão, Perfis compósitos, Fluência, Durabilidade

# 1- INTRODUCTION

The presence of fiber reinforced polymers (FRP) in profiles for structures is becoming more relevant in construction and rehabilitation of existing structures. The fabrication of normalized beams in FRP is the consequence of the properties that this family of materials presents: being lightweight, noncorrosive, possessing high specific strength and stiffness, ease of construction, and tailor-made to satisfy the necessary performance requirements. Another important characteristic of the FRP is its long-lasting properties. The lightweight that is intrinsic to an FRP allows for cost-effective construction (Lee and Jain, 2009). In the case of emergencies or disaster, rapid availability and reliability is the key. Composite structures made of glass fiber reinforced polymer (GFRP) profiles are especially suitable due to their characteristic manoeuvrability, lightweight and the well-known manufacturing parameters of the pultrusion process (Cavaleri et al., 2019; Liu et al. 2021).

The use of GFRP pultruded profiles in structures subject to harsh environments is one of the most important applications of those materials, as traditional materials often are sensitive to conditions such as frequent freezing cycles and salts (Jafari et al. 2019; Verdenikov et al. 2020).

Despite the advantages of using thermosetting FRPs, the fact that these present low ductility, low shear strength, vulnerability to extreme temperatures and possible degradation of mechanical properties when exposed to alkaline environments, UV radiation, temperature cycles and fluctuating hydrothermal conditions can pose some obstacles to the use of these materials in civil construction (Jafari et al., 2019).

The lifetime of composite structural elements is strongly influenced by temperature and time-dependent behaviour of the matrix (Yang et al. 2018):

- Low temperatures may cause the plastic to become brittle and may induce cracking and propensity to fracture;
- Elevated temperatures may result in degradation of mechanical properties, cracking, chalking and flaking of polymers;
- Cyclic exposure may cause interfacial debonding and matrix cracking;
- Stress relaxation and creep will occur when a viscoelastic material is exposed to quasi-static loading and load changes.

In a study by Pour-Ghaz et al. (2016), the maximum tensile strength lost by GFRP was 30% for specimens aged 224 days at 55°C. The application of loads at high temperatures showed that specimens lost 35% of the tensile strength and a high debonding in the fiber/matrix interface was noticed.

It was shown that there is no synergetic effect on the degradation rate of GFRP between mechanical and environmental loading at a given stress level. Therefore, there is no correlation between the sustained stress level and the rate of degradation of the mechanical properties. This test applied a load level of 30% of the ultimate tensile strength (Pour-Ghaz et al., 2016).

Water may induce physical and/or chemical aging. This aging can be partially reversible, reversible or irreversible depending on the nature of the material and period of conditions exposed. Working humidity conditions imply water absorption with weight changes happening the most (Kafodya et al. 2015).

Flexural strength is strongly affected by water absorption due to polymer degradation. This effect is accelerated by temperature. UV radiation mainly causes surface deterioration increasing the risk of humidity and other agents. As such, profiles in GFRP should contain a certain protective coating thickness to prevent the effect of UV radiation. Therefore, UV radiation has a small influence on the mechanical properties of the structural element having a bigger effect on the aesthetic and surface properties (Correia et al., 2016).

Regarding different matrix materials, the study conducted by Carra and Carvelli (2015) showed that E-glass reinforced vinylester retained flexural strength more effectively than isophthalic polyester and ortophtalic polyester matrices. For an average service temperature of 23°C, it showed that vinylester matrices hold 65% of the original value of flexural properties for more than 100 years whilst isophthalic polyester holds for 75 years and ortophtalic polyester can keep 65% of the properties for about 20 years (Carra and Carvelli, 2015).

The study conducted by Jafari et al. (2019) studied the effects of thermal cycles on the mechanical response of GFRP pultruded profiles made of E-glass fiber and vinylester. I-shaped and U-shaped profiles were tested for temperature cycles between -20°C and 20°C. It was concluded (Jafari et al., 2019) that:

- Profiles with a larger cross-section exhibit better mechanical performance after thermal cycles;
- I-beam and U-beam profiles show better strength retention when tested along their principal weak axis rather than their strong axis. The thermal cycles have a major effect on the resin matrix, but an insignificant effect on the glass fibers;
- After exposition to thermal cycles, GFRP profiles present higher strength retention in tension than in compression;
- Although thinner laminates have a higher tensile strength due to their higher fiber density, thicker laminates exhibit a better durability performance.

The study conducted by Bazli et al. (2020) analysed the effects of UV radiation, moisture and elevated temperature on the mechanical properties of GFRP pultruded profiles made of E-glass and vinylester. This study concluded that after up to 3000h of UV radiation and water vapour condensation cycles, the mechanical properties of various GFRP sections generally decreased, having a lower rate of increase up to 1000h, a rapid increase from 1000h to 2000h and a slow increase again until 3000h of testing. The maximum reductions in properties were around 30% for bending, tensile and compression tests (Bazli et al., 2020).

## 2- MATERIALS AND METHODS

The material is a rectangular pultrusion profile with a cross-section of 30x5mm<sup>2</sup> consisting of an ortophtalic polyester matrix reinforced with E-glass fiber.

This work is divided in three stages, namely:

- Stage 1: Flexural tests to obtain the mechanical properties of the material
- Stage 2: Flexural creep tests at different load levels
- Stage 3: Flexural creep test of samples subject to immersion in tap water.

## 2.1. Stage 1

Stage 1 aims at characterizing the mechanical properties of the material as a reference for the subsequent creep tests. For the flexural test, the length of the specimens was 200mm and the span length  $L$  was 150mm. The test velocity was 1mm/min. The test setup is shown in Figure 1. The standard EN13706-2 (EN13706-2, 2002) was used as a reference for the three-point bending tests.

## 2.2. Stage 2

From the results of stage 1, the failure load was measured. In this stage, the time-to-failure of specimens was measured at 50%, 60%, 70% and 75% of the failure load. During these creep tests, the vertical displacement of each specimen was measured. The same span length was used as in stage 1,  $L = 150\text{mm}$ .

At this stage, the creep behaviour is described by a linear Findley's model (1),

$$\frac{\varepsilon(t)}{\sigma_0} = J(t) = \frac{1}{E_0} + \frac{1}{E_t} t^n \quad (1)$$

where  $\varepsilon(t)$  represents the long-term strain,  $J(t)$  the creep compliance,  $E_0$  - initial elastic modulus, and  $E_t$  and  $n$  the stress-independent parameters (Cardoso and Harries, 2019).

This linear Findley's model is stress independent, meaning that the same law should be obtained regardless of the load level (Sá et al., 2011). The model separates the compliance components into a time-dependent and a time-independent component.



Fig. 1 | Three-point bending test setup

### 2.3. Stage 3

Specimens were submerged in tap water for 480h and then subject to flexural creep tests at 70% and 75% of the failure load obtained for pristine specimens. The test setup is the same as in Stage 2.

## 3- RESULTS AND DISCUSSION

### 3.1. Stage 1

The results of the flexural tests are shown in Table 1. The flexural modulus did not correlate well to the modulus indicated by the supplier which is 23GPa, the reason being the span-to-depth ratio which was lower than the recommended 60:1 of the standard ASTM D790.

Table 1 | Results of the flexural tests

|           | $E_f$<br>[GPa] | $\sigma_r$<br>[MPa] | $\epsilon_r$ | $F_{max}$<br>[N] |
|-----------|----------------|---------------------|--------------|------------------|
| 1         | 52.65          | 661                 | 0.015        | 2204             |
| 2         | 54.00          | 661                 | 0.014        | 2204             |
| 3         | 56.93          | 671                 | 0.013        | 2238             |
| $\bar{x}$ | 54.53          | 665                 | 0.014        | 2215             |

### 3.2. Stage 2

Figure 2 displays the strain plotted against time for 65%, 70% and 75% of the maximum load. From the current test results data, it can be observed that the strain evolution for the sample of 65% loading was slower than the 70% and 75% respectively. In addition, this sample took more time to fail.

On the other hand, the samples with 75% and 70% loading, were similar in terms of strain

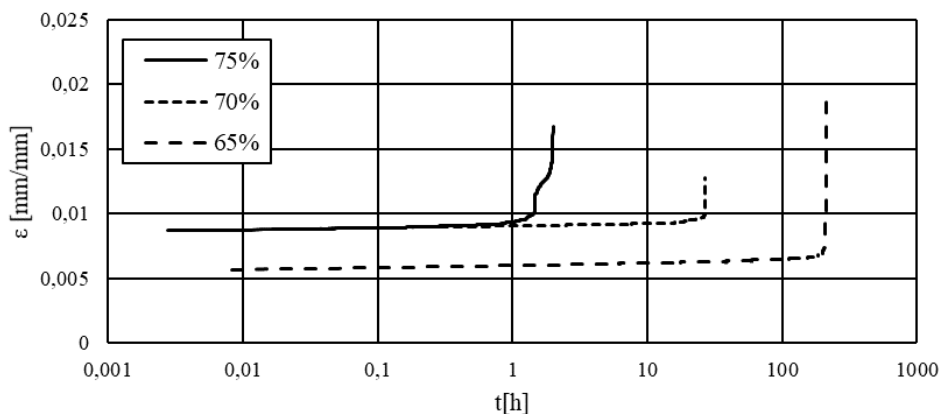


Fig. 2 | Short-term creep tests on specimens subject to 65%, 70% and 75% of the maximum load

achieved before catastrophic failure. However, the sample with 70% loading, as expected, took more time to fail.

Figure 2 shows that for an increase of 5% in the load, the respective time until failure reduced approximately by a factor of 10. Such phenomenon can be better observed by plotting stress versus the time that led to catastrophic failure, Figure 3. The exponential function describes well this behavior:

$$t[h] = 3 * 10^{15} e^{-0,07\sigma_f} \quad (2)$$

where  $\sigma_f$  is the flexural stress.

Additionally, a sample was tested at 50% of the maximum load. The results from this test are shown in Figure 4. This specimen has the test interrupted before it failed, due to time limitations. The results of this test were used to curve fit the creep compliance using equation (1).

Approximating the compliance of the specimen tested at 50% of the maximum load with the Findley's model, the following law in equation (3) was obtained.

$$\frac{\varepsilon(t)}{\sigma_0} = J(t) = \frac{1}{38.07} + \frac{1}{1797} t^{0.18} \quad (3)$$

From the equation, the following values can be consulted: the initial flexural modulus was 38.07 GPa the material parameter  $E_t$  for the creep compliance prediction was 1797GPa and the coefficient  $n$  was 0.18. These values are coherent with the literature (Cardoso and Harries, 2019) where values for  $E_t$  and  $n$  have been reported to be between 500 and 3700 GPa and; 0.15 and 0.36 respectively. The initial modulus  $E_0$  is lower than the measured flexural modulus, however, when evaluating figure 2, the model correlation is weaker in the first stage of creep, which can cause this lower value.

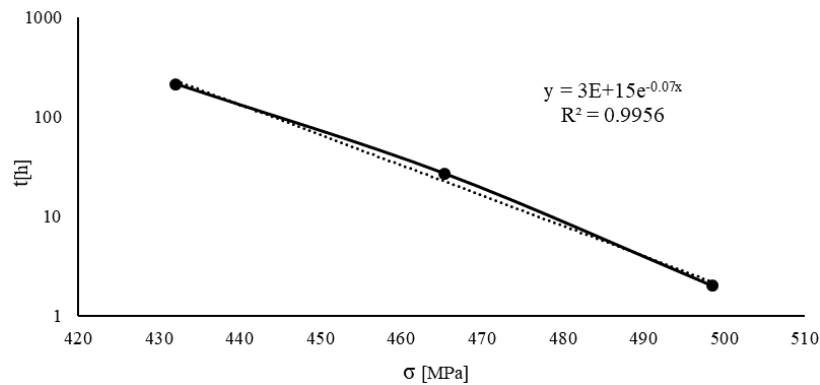


Fig. 3 | Experimental modelling of time to failure based on the three specimens.

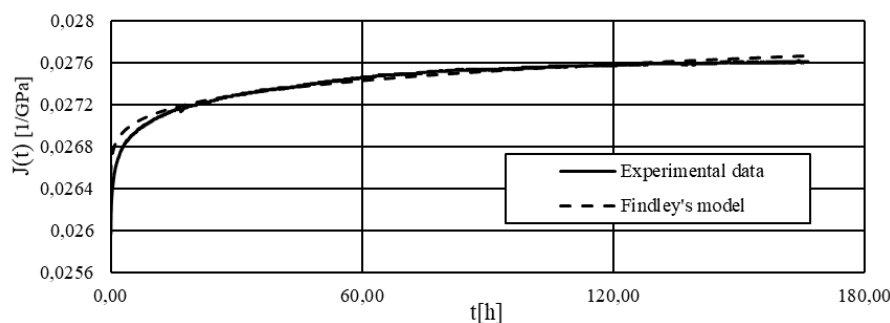


Fig. 4 | Flexural creep test at 50% of the maximum force and correlation with Findley's model

Using equation (2), nearly 27 years would be necessary for the specimen at subject to 50% of the maximum load to reach rupture. This prediction should be considered with some caution since only one sample was tested for each load.

### 3.3. Stage 3

When designing a structure, it is of utmost importance to have environmental factors in mind. Since these structures are often exposed to those environmental factors, it becomes relevant to study the influence of humidity on the mechanical properties of the components. Figure 5 displays the strain curve for the sample with the 70% and 75% loads, for dry and wet samples. Regarding the data it is possible to observe that catastrophic failure of the wet specimen for the load of 75% occurred 10 times before the respective dry sample. A similar situation is seen for 70% of the samples.

Commonly used as a method to predict the life properties of composite systems is the time-temperature superposition (TTSP) method. Due to the polymeric sensitivity to environmental conditions, this method employs different test temperatures, to accelerate the creep rate. This way it is possible to study the viscoelastic behaviour over the entire service lifetime (Houhuou et al., 2014).

Therefore, in this method, creep compliance will be a function of temperature and time. The master curve will be created by shifting horizontally along the log-time axis of the samples using a shift factor (Houhuou et al., 2014). This shift factor can be determined from the Williams-Landel-Ferry equation (Williams et al., 1955):

$$\log(\alpha_T) = \frac{-C_1(T-T_0)}{C_2+(T-T_0)} \quad (4)$$

Houhuou et al. (2014) showed that each short-term creep test, took an hour, with 30 minutes of creep loading followed by 30 minutes of creep-recovery. The temperatures ranged from 25°C to 57°C with a variation of 2°C.

Thus, in 960 minutes or 16 hours, it was possible to accurately create a master creep curve for  $10^{13}$  presenting a less time-consuming method, that therefore can lead to more accurate properties, allowing to test more samples.

Therefore, for future works, it is suggested to use the TTSP methodology starting with a room

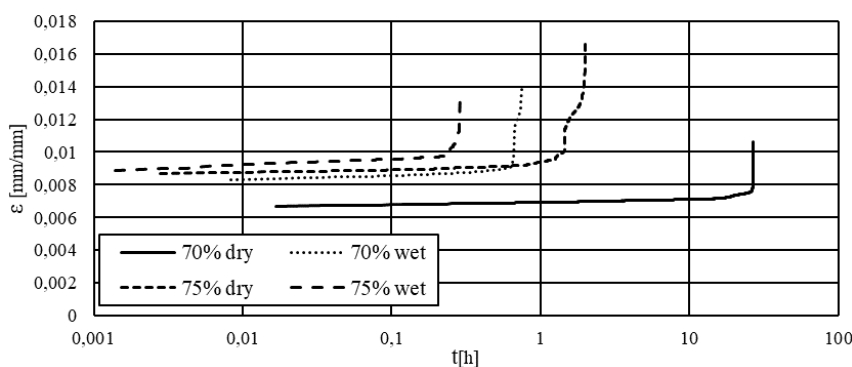


Fig. 5 | Short term creep test on wet specimens, tested at 70% and 75% of the maximum load

temperature test up near to the matrix glass transition temperature. Stress levels also need to be taken into consideration, as shown by Houhuou et al. (2014). Higher stress levels will shift the master curve to shorter times and drop the creep compliance at failure.

## 4- CONCLUSIONS

This work consisted of three stages of study of pultruded GRFP profiles where two main aspects were developed. The first being a prediction of the lifetime of the structure, by developing a correlation between the flexural stress and the time-to-failure for this specific material and profile geometry.

As a measure of property loss, the results of the creep tests were approximated with Findley's model. Thus, it is possible to approximate the flexural strain for a given load level.

Additionally, it was studied how water absorption can damage the properties of the material. Even though GFRP present better corrosion properties than other structural materials, water absorbed by the orthophthalic polyester matrix can decrease the resistance of the material.

Finally, this study aided in the conclusion that the fiber/matrix interface is extremely important since the parts failed due to debonding leading to delamination, as can be seen in Figure 6. This behaviour can be seen in parts that are dry and parts subjected to water absorption.



Fig. 6 | Debonding and delamination in the parts

## ACKNOWLEDGEMENTS

The authors would like to acknowledge ALTO perfis in providing the material for the experimental tests.

## REFERENCES

- Bazli, M., Jafari, A., Ashrafi, H., Zhao, X.-L., Bai, Y., and Raman, R. S. (2020). Effects of UV radiation, moisture and elevated temperature on mechanical properties of GFRP pultruded profiles. *Construction and Building Materials*, 231:117137.
- Cardoso, D. C. T. and Harries, K. A. (2019). A viscoelastic model for time-dependent behavior of pultruded GFRP. *Construction and Building Materials*, 208:63 - 74.
- Carra, G. and Carvelli, V. (2015). Long-term bending performance and service life prediction of pultruded glass fibre reinforced polymer composites. *Composite Structures*, 127:308 - 315.
- Cavaleri, L., Paola, M. D., Ferrotto, M., Scalici, T., and Valenza, A. (2019). Structural performances of pultruded GFRP emergency structures – part 1: Experimental characterization of materials and substructure. *Composite Structures*, 214:325 - 334.
- Correia, J. R., Cabral-Fonseca, S., Branco, F. A., Ferreira, J. G., Eusébio, M. I., and Rodrigues, M. P. (2006). Durability of pultruded glass-fiber-reinforced polyester profiles for structural applications. *Mechanics of Composite Materials*, 42(4):325-338.
- EN13706-2. Reinforced plastics composites . Specifications for pultruded profiles - Part 2: Methods of test and general requirements. CEN: Brussels, Belgium; 2002.
- Houhou, N., Benzarti, K., Quiertant, M., Chataigner, S., Fléty, A., & Marty, C. (2014). Analysis of the nonlinear creep behavior of concrete/FRP-bonded assemblies. *Journal of adhesion science and technology*, 28(14-15), 1345-1366.
- Jafari, A., Ashrafi, H., Bazli, M., and Ozbakkaloglu, T. (2019). Effect of thermal cycles on mechanical response of pultruded glass fiber reinforced polymer profiles of different geometries. *Composite Structures*, 223:110959.
- Kafodya, I., Xian, G., Li, H., Durability study of pultruded CFRP plates immersed in water and seawater under sustained bending: Water uptake and effects on the mechanical properties
- Lee, L. S. and Jain, R. (2009). The role of FRP composites in a sustainable world. *Clean Technologies and Environmental Policy*, 11(3):247–249.
- Liu, TQ, Feng, P. et al., Developing an innovative curved-pultruded large-scale GFRP arch beam, *Composite Structures*, 256 (2021.01.15),113111, doi.org/10.1016/j.compstruct.2020.113111
- Pour-Ghaz, M., Miller, B. L., Alla, O. K., and Rizkalla, S. (2016). Do mechanical and environmental loading have a synergistic effect on the degradation of pultruded glass fiber reinforced polymers? *Composites Part B: Engineering*, 106:344 - 355.
- Sá, M. F., Gomes, A. M., Correia, J. R., and Silvestre, N. (2011). Creep behavior of pultruded gfrp elements - part 1: Literature review and experimental study. *Composite Structures*, 93(10):2450 - 2459.
- Williams, M. L., Landel, R. F., & Ferry, J. D. (1955). The temperature dependence of relaxation mechanisms in amorphous polymers and other glass-forming liquids. *Journal of the American Chemical society*, 77(14), 3701-3707.
- Vedernikov, A., Safonov, A., Tucci, F., Carlone, P., Akhatov, I., Pultruded materials and structures: A review, *Journal of Composite Materials* 2020, Vol. 54(26) 4081–4117
- Yang, Z., Wang, H., Ma, X., Shang, F., Ma, Y., Shao, Z., and Hou, D. (2018). Flexural creep tests and long-term mechanical behavior of fiber-reinforced polymeric composite tubes. *Composite Structures*, 193:154 - 164.